IEEE Photonics Journal
An IEEE Photonics Society Publication

Open Access

Digital Code-Division Multiplexing Channel Aggregation for Mobile Fronthaul Architecture With Low Complexity

Volume 10, Number 2, April 2018

Haibo Li
Qi Yang
Songnian Fu
Ming Luo
Xiang Li
Zhixue He
Peng Jiang
Yongpiao Liu
Shaohua Yu

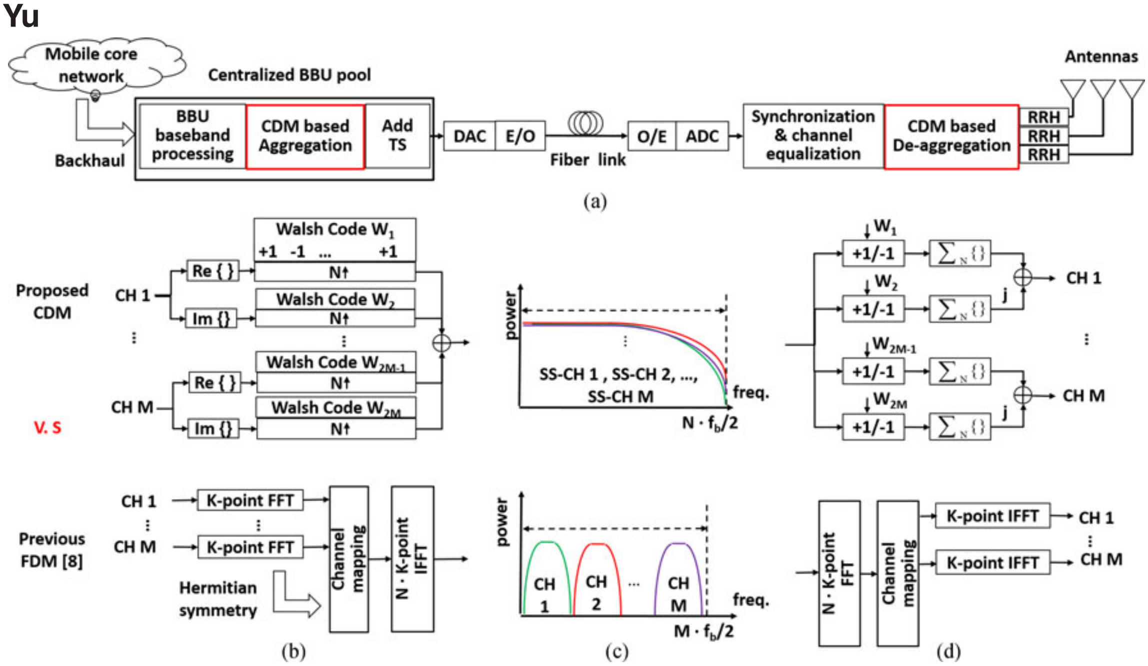

DOI: 10.1109/JPHOT.2017.2751538

Digital Code-Division Multiplexing Channel Aggregation for Mobile Fronthaul Architecture With Low Complexity

Haibo Li,[1,2] Qi Yang,[2] Songnian Fu,[1] Ming Luo,[1,2] Xiang Li,[2] Zhixue He,[2] Peng Jiang,[3] Yongpiao Liu,[3] and Shaohua Yu[1,2]

[1]Wuhan National Laboratory for Optoelectronics & School of Optical and Electronic Information, Huazhong University of Science and Technology, Wuhan 430074, China
[2]State Key Laboratory of Optical Communication Technologies and Networks, Wuhan Research Institute of Posts & Telecommunications, Wuhan 430074, China
[3]Wuhan Hongxin Telecommunication Technologies Co., Ltd., Wuhan 430074, China

DOI:10.1109/JPHOT.2017.2751538

Manuscript received May 16, 2017; revised September 1, 2017; accepted September 6, 2017. Date of publication September 12, 2017; date of current version April 10, 2018. Corresponding author: H. Li (e-mail: hbli@wri.com.cn).

Abstract: A low-complexity mobile fronthaul architecture via digital code-division multiplexing (CDM) is proposed to enable channel aggregation of 4G-LTE signals. In comparison with traditional frequency division multiplexing based aggregation scheme, the fast Fourier transformation/inverse fast Fourier transformation operations are replaced by simple sign selection and addition, leading to the significant reduction of computational complexity. Moreover, synchronous transmission of both the I/Q waveforms of wireless signals and the control words (CWs) used for the purpose of control and management using the CDM approach is also presented to be compliant with the common public radio interface (CPRI). In a proof-of-concept experiment, we demonstrate the transmission of 48 $\times$ 20 MHz LTE signals with CPRI equivalent data rate of 59 Gb/s, achieving an average error vector magnitude (EVM) of $\sim$3.6% and $\sim$4.3% after 5 and 20 km transmission over standard single-mode fiber (SSMF), respectively. Furthermore, we successfully demonstrate the transmission of 32 $\times$ 20 MHz LTE signals together with CPRI-compliant CWs, corresponding to CPRI-equivalent data rate of 39.32 Gb/s, only using single optical wavelength channel with analog bandwidth of $\sim$1.96 GHz. After transmission over 5 km SSMF, CWs can be error-free recovered while the LTE signals are recovered with an EVM of $\sim$3.6%.

Index Terms: Mobile fronthaul, digital code-division multiplexing (CDM), control words (CWs).

1. Introduction

As an attractive next-generation wireless network , centralized radio access network (C-RAN) offers several benefits, in term of both network energy efficiency and network performance via coordinated multi-point [1], [2]. In C-RAN, the optical links between centralized baseband units (BBUs) and remote radio heads (RRHs) constitute the mobile fronthaul (MFH), which primarily employ a digital optical communication method based on interfacing technologies such as a common public radio interface (CPRI) [3], [4]. However, CPRI is not bandwidth-efficient due to the use of binary modulation from quantized signal. For instance, using CPRI, the 3 GPP release-13 requires 320-Gbps bandwidth for a single RRH without sectoring, and nearly 1-Tbps with 3 sectors [3]. To increase the bandwidth efficiency of MFH, transmission of multiple channel mobile signals employing frequency division multiplexing (FDM) based channel aggregation has been widely studied. Basically, these channel aggregation schemes can be divided into two categories: 1) analog signal processing that includes frequency conversion and radio frequency (RF) combining/splitting [5]; 2) digital FDM aggregation by digital signal processing (DSP) via fast Fourier transformation/inverse fast Fourier transformation (FFT/IFFT) [6]–[8]. Compared to the analogue FDM aggregation scheme, high performance and flexible implementation could be achieved by using the DSP-based solutions [6]. However, the computational complexity of the digital FDM aggregation will be huge, because the large size FFT/IFFT is required for multiple-channel aggregated signals. Even though the frequency-domain windowing (FDW) technique is employed to reduce the size of the FFT/IFFT needed for channel aggregation and de-aggregation [7], a lot of multiplication operations introduced by FFT/IFFT and FDW are still inevitable. As another type of multiplexing technology, code division multiplexing (CDM) employs spread-spectrum technology and a special coding scheme (where each sub-channel is assigned a code) to allow multiple channels to be multiplexed over the same frequency bandwidth [9]. CDM has been widely employed in both wireless and optical communications due to its several instinctive benefits, such as networking versatility, anti-interference, high security and low cost implementation [10]–[12]. But no applications has been investigated in the mobile fronthaul, to the best of our knowledge.

In this paper, we propose a digital CDM channel aggregation for mobile fronthaul with low complexity, and employ the training sequence based channel equalization [13] to compensate the channel response for the aggregated signal. Different from FDM based aggregation scheme [6]–[8], the FFT/IFFT operations are replaced by simple sign selection and addition, leading to the significant reduction of computational complexity. The proposed MFH architecture is experimentally verified by aggregating 48 $\times$ 20-MHz long term evolution (LTE) signals, achieving a CPRI-equivalent data rate of 59-Gb/s, over single-wavelength channel with analog bandwidth of 1.966-GHz. An average error vector magnitude (EVM) of $\sim$3.6 % and $\sim$4.3% is achieved after transmission over 5-km and 20-km standard single-mode fiber (SSMF), respectively. In order to make the CDM-based aggregation approach compatible with the CPRI interface, additional transmission of the control words (CW) is compulsory. Thus, a novel mobile fronthaul transmission scheme is experimentally demonstrated to achieve the transmission of 32 $\times$ 20-MHz LTE signals together with CPRI-compliant CWs, corresponding to CPRI-equivalent data rate of 39.32-Gb/s. After transmission over 5-km SSMF, the CWs are recovered without error, while the LTE signals are recovered with an EVM of $\sim$3.6%.

2. Operation Principle

Fig. 1(a) shows the schematic diagram of proposed MFH architecture using DSP-based channel aggregation and de-aggregation via CDM. In the centralized BBU pool, mobile signals after baseband processing are aggregated using the proposed CDM scheme, which is described in details later. Then, the aggregated signals are added with training sequences (TS) for synchronization and channel estimation [13], and converted to an analog signal. The electronic analog signal is then converted to optical signal and transmitted through fiber link. At the received side, TS-based synchronization and channel equalization is firstly conducted to compensate the channel response for the aggregated signal. Then, multiple baseband signals are retrieved via CDM based de-aggregation and delivered to RRHs. To specify the process and superiority of the proposed CDM based aggregation, we carry out a comparison between the proposed CDM scheme and the previous FDM scheme [6]–[8]. As shown in Fig. 1(b), FDM based aggregation scheme divides the available frequency bandwidth into a series of non-overlapping sub-bands in order to carry each mobile signal separately via FFT/IFFT operations [8]. It is worth noting that, the FFT/IFFT operations will inevitably introduce a lot of multiplications. By contrast, the proposed CDM based aggregation employs spread-spectrum technology via Walsh code [14] (where each aggregated mobile signal is assigned a pair of code sequence) to allow multiple mobile signals to be multiplexed over the same frequency bandwidth via only sign selection and addition operations. More specifically, each input complex mobile signal is firstly separated into real part and imaginary part. Each sample is then

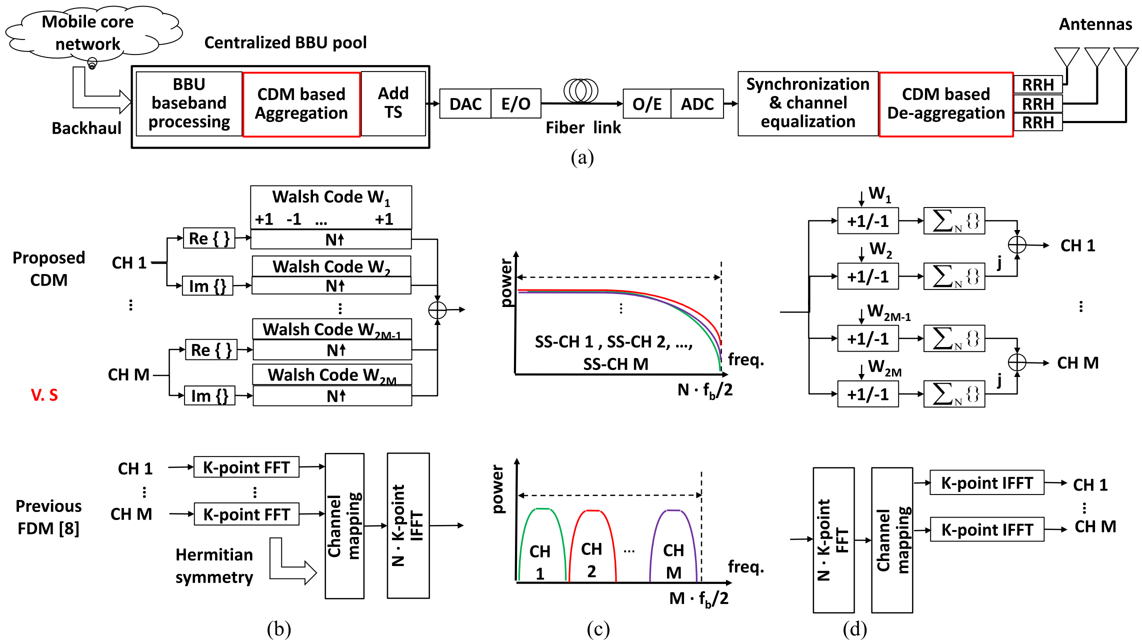

Fig. 1. (a) Schematic diagram of MFH architecture using DSP-assisted channel aggregation and de-aggregation via CDM. (b) Comparison of DSP flow for proposed CDM-based aggregation and previous FDM-based aggregation. (c) Comparison of schematic frequency spectrums of the aggregated signal via CDM and FDM. (d) Comparison of DSP flow for CDM-based de-aggregation and FDM-based de-aggregation.

repeated by a factor of N, where N ($= 2^n$, n is a positive integer) denotes the order of Walsh code, and the number of aggregated mobile channels is denoted as M ($2M \leq N$). Then, a pair of Walsh code sequence denoted as w_{2k-1} and w_{2k} ($k = 1, 2 \ldots, M$) composed of $+1/-1$ is employed to determine the signs of repeated samples. Next, all the spread spectrum coding signals are summed together as the aggregated signal. The schematic spectrums of the aggregated signal via CDM and FDM are also compared as shown in Fig. 1(c). When M is not a power of two, $2M < N$ is satisfied. Thus, the bandwidth of aggregated signal via CDM is a little larger than that of FDM. The reverse process of the CDM and FDM aggregation is applied to recover the original mobile signals, as shown in Fig. 1(d). The DSP process of aggregation and de-aggregation can be implemented only using sign selection and addition/subtraction operations for CDM. The proposed CDM based approach offers a key benefit: compared to FDM scheme, none multiplications is required. Thus, the computational complexity can be greatly reduced.

To facilitate the control and management of the fronthaul equipment with CPRI, it is necessary to transmit the CWs together with the wireless signals [15]. The schematic setup of the CDM-based channel aggregation and de-aggregation with the transmission of both wireless signals and CWs is shown in Fig. 2. The M digital baseband signals are firstly spread spectrum coding by M pairs of N-order Walsh code. Meanwhile, the CW bits are modulated via quadrature amplitude modulation (QAM). The QAM signals are then passed through a 1: K serial-parallel conversion (S/P). The value K is the ratio between the baud rate of the QAM signals and that of each LTE signals. Each parallel QAM signal is separated into real part and imaginary part, and then repeated by N. Then, a pair of Walsh code sequence denoted as $w_{2k-1,\ K}$ and $w_{2k,\ K}$ ($k = 1, 2 \ldots, K$) composed of $+1/-1$ is employed to determine the signs of repeated samples. Finally, all the spread spectrum coding LTE and QAM signals are summed up as an aggregated signal. The reverse process of the CDM aggregation is applied to recover the original LTE signals and CWs as shown in Fig. 2(b).

To maintain a bit error ratio (BER) of $< 10^{-12}$ for the CWs [4], 16-QAM is chosen for CWs modulation and the baud rate needed for CWs is ½ of that needed for LTE signals [8].

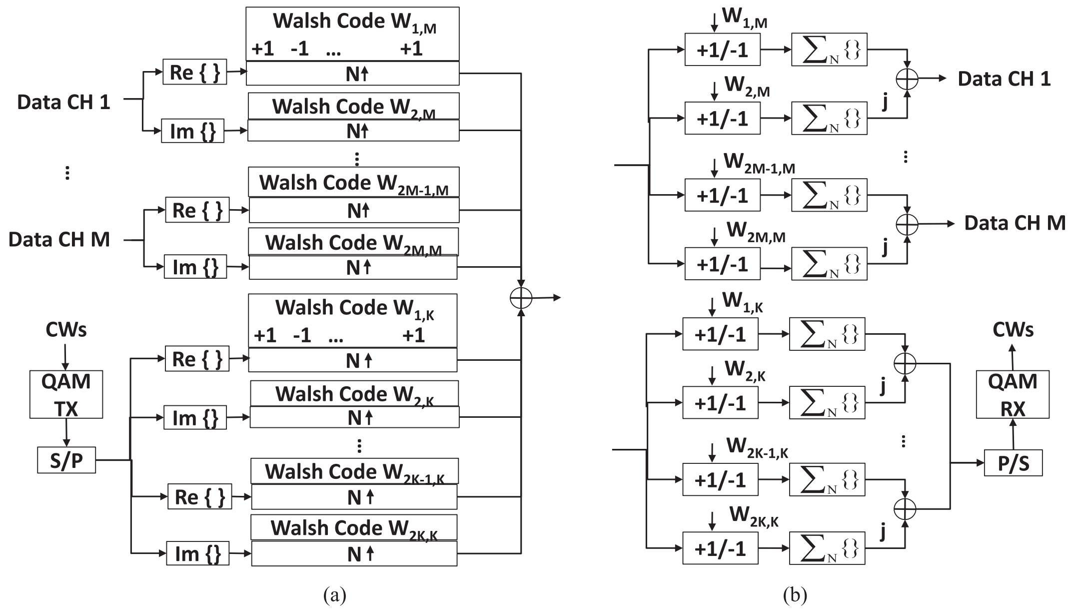

Fig. 2. DSP flow of CDM-based (a) aggregation and (b) de-aggregation with the transmission of both wireless signals and CWs.

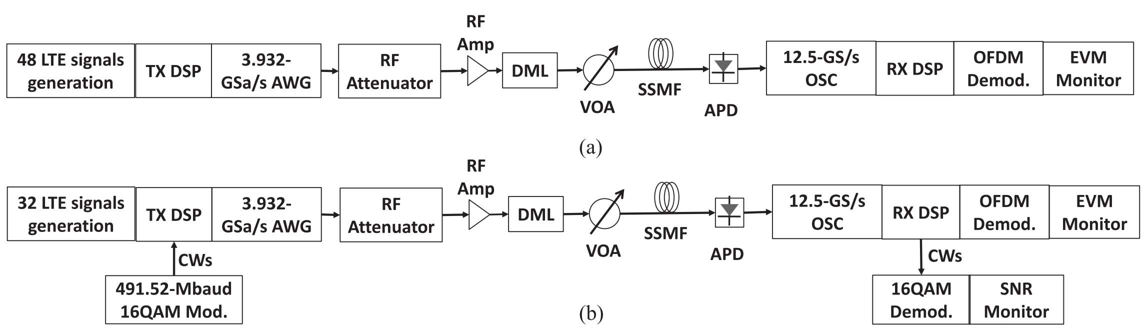

Fig. 3. (a) Experimental setup of 48 $\times$ 20 MHz-LTE signal transmission by digital CDM-based channel aggregation. (b) Experimental setup for the synchronous transmission of 32 $\times$ 20 MHz-LTE signals and CWs sampled at 491.52 MHz by digital CDM-based channel aggregation.

3. Experimental Setup

Fig. 3(a) shows the experimental setup for the MFH transmission using CDM-based aggregation. At the transmitter, a representative macro-cell with 48 $\times$ 20-MHz LTE signals, each having a sampling rate of 30.72 MHz, is firstly generated with offline DSP. The modulation format is orthogonal frequency division multiplexing (OFDM) with 64-QAM, which is the highest modulation level specified in LTE. Then, 48-channel LTE signals are aggregated by the proposed CDM aggregation scheme with 128-order Walsh code and outputed by an arbitrary waveform generator (AWG) operated at 3.932-GSa/s. RF attenuator and microwave amplifier are employed to adjust the optical modulation index (OMI) of the used directly modulated laser (DML) [16]. Next, we build up traditional single-wavelength intensity modulation direct direction (IM-DD) link, including a 1550-nm 10 G-class DML, a variable optical attenuator (VOA), 20-km SSMF, and a commercial 10-GHz avalanche photodiode (APD). The detected signal is digitized by a real-timing oscilloscope (OSC) working at 12.5-GS/s, and consequent processed with the offline DSP for channel de-aggregation, OFDM demodulation, and EVM evaluation. For performance comparison, the FDM aggregation scheme [8] is also conducted under the same photonic link configuration.

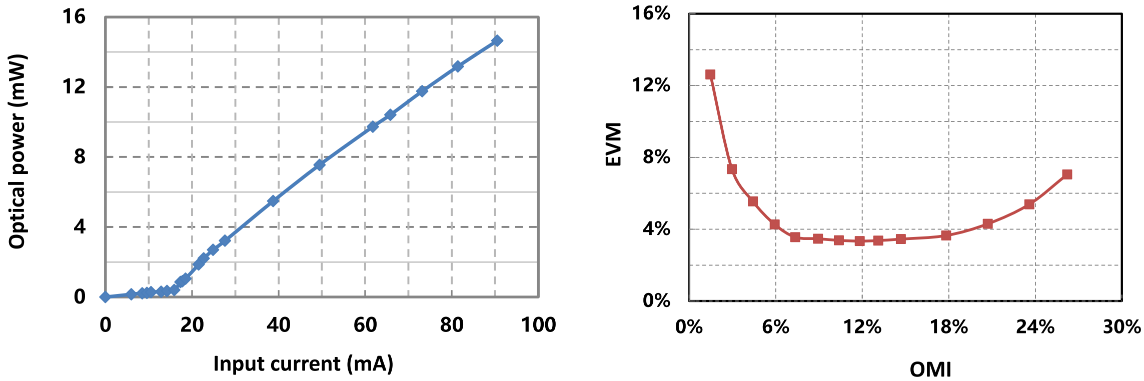

(a) (b)

Fig. 4. (a) P-I curve of used DML (b) Mean EVM performance of 48 LTE signals using CDM as a function of OMI under the condition of back-to-back fiber optical transmission.

Fig. 3(b) shows the experimental setup for the synchronous MFH transmission of LTE signals and CWs. We first generate 32 $\times$ 20-MHz LTE signals with OFDM modulation by 64-QAM subcarrier, and a 491.52-Mbaud 16-QAM signal to carry the CWs. Those signals are then aggregated via CDM as described in Fig. 2(a). After the same single-channel photonic link as shown in Fig. 3(a), the detected signal is digitized by OSC working at 12.5-GS/s, and later processed as shown in Fig. 2(b). The received OFDM-64 QAM signal is evaluated by EVM, and the coresponding 16-QAM signal is evaluated by received signal-to-noise ratio (SNR).

4. Results and Discussions

To make the DML operate at optimal condition, we evaluate the mean EVM performance of all 48 LTE signals using CDM as a function of OMI under the condition of back-to-back fiber optical transmission. Generally, OMI is defined as $OMI = V_{in}/[(I_{bias} - I_{th})R]$ [17], where R is the internal resistance of DML, V_{in} is the input RF voltage of DML, I_{bias} is the bias current, and I_{th} is the threshold current. To verify the threshold current and the bias current of DML, we firstly measure the P-I curve of the used DML. As shown in Fig. 4(a), when the input current is below 18 mA, the laser output mainly comes from spontaneous emission. When the input current increases more than 18 mA, the output power of DML has a linear relationship with respect to the input current. Therefore, the threshold current of the DML is estimated as 18 mA. The maximum input current is around 90 mA. Please note that the maximum input current of DML is limited to less than 95 mA in order to protect the device. Thus, we choose the bias current I_{bias} as 54 mA. The internal resistance of DML is $\sim$75 Ω according to the datasheet. Then, we can employ the RF attenuator and microwave amplifier to manage the input RF voltage V_{in} of DML. The corresponding OMI is continuously adjusted. As shown in Fig. 4(b), the transmission performance at a low OMI is limited by shot noise mainly. Meanwhile, performance degradation still occurs at a high OMI because of clipping distortion at the nonlinear region. The dynamic range of OMI with minimum EVM is around 9%$\sim$14%, and the corresponding input RF power of DML is around $-1.1\sim3.1$d Bm. Thus, the OMI of 11% is set for the rest of our experiments.

Fig. 5(a) shows the mean EVM of all 48 LTE signals with respect to the received optical power. We firstly compare the EVM performance for CDM and FDM, under the scenario of back-to-back (B2B, $L = 0$ km) transmission. As shown in Fig. 5(a), almost the same performance can be secured via CDM based aggregation, in comparison with the FDM based aggregation. However, the total DSP complexity is greatly reduced, because the involved FFT/IFFT operation for FDM is replaced by simple addition/subtraction and accumulation operations for CDM. The computational complexity evaluated as the number of real addition and multiplication is also shown in Table 1. In general, the number of complex addition and complex multiplication for each N-point IFFT operation is $N\log_2 N$

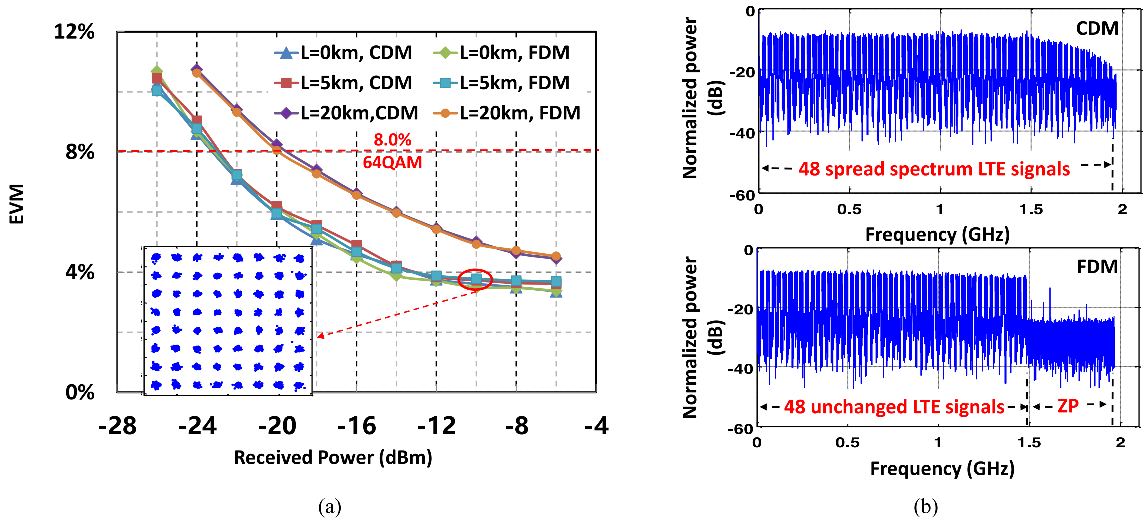

Fig. 5. (a) Mean EVM of the aggregated 48 × 20 MHz-LTE signals versus received optical power via FDM-based aggregation (L = 0 km), FDM-based aggregation (L = 5 km), FDM-based aggregation (L = 20 km), CDM-based aggregation (L = 0 km), CDM-based aggregation (L = 5 km) and CDM-based aggregation (L = 20 km), respectively. (b) Measured RF spectrum prior to channel de-aggregation for CDM and FDM, respectively

TABLE 1

Comparison of Computational Complexity for CDM and FDM

	Real addition	Real multiplication
FDM	153600	102400
CDM	389120	0

and $(N\log_2 N)/2$, respectively. One complex multiplication requires 4 real multiplications and 2 real additions, and one complex addition requires 2 real additions. According to the FFT/IFFT size and the number of aggregated channels, the required number of real additions and real multiplications for FDM could be estimated as 153600 $(= 48 \times 2 \times 3 \times 16 \times \log_2(16) + 2 \times 3 \times 2048 \times \log_2(2048))$, and 102400 $(= 48 \times 2 \times 2 \times 16 \times \log_2(16) + 2 \times 2 \times 2048 \times \log_2(2048))$, respectively. The proposed CDM based aggregation scheme requires more real additions of 389120 $(= 128 \times (48 \times 2 - 1) \times 16 \times 2)$. However, the required number of real multiplications is 0 for the proposed CDM scheme. It is worth noting that, the complexity of the real multiplication is severe than that of the real addition, even though a lot of algorithm have been proposed to reduce the complexity of multiplication [18]. Therefore, the computational complexity of the CDM scheme is greatly reduced in comparison with that of the FDM scheme. Fig. 5(b) shows a measured RF spectrum before channel de-aggregation for CDM and FDM, respectively. Clearly, the electrical spectrum is within ~1.966 GHz for CDM, which is 64 times of 30.72 MHz, and the sampling rate is thus 3.932 (= 1.966 × 2) GSa/s. For FDM, the electrical bandwidth of 48 unchanged LTE signals is around 1.5 GHz and zeros padding (ZP) is required due to oversampled IFFT is employed. Therefore, the required sampling rate is the same as that of CDM, i.e., 3.932 GSa/s. We further conduct CDM and FDM based aggregation under 5-km (L = 5 km) and 20-km (L = 20 km) SSMF transmission, respectively. When L = 5 km, very slight performance degradation is observed compared to the results of B2B transmission, indicating of negligible fiber dispersion induced penalty for both CDM and FDM scheme. Since the required EVM threshold is 8% for 64-QAM, the received optical power needs to be larger than

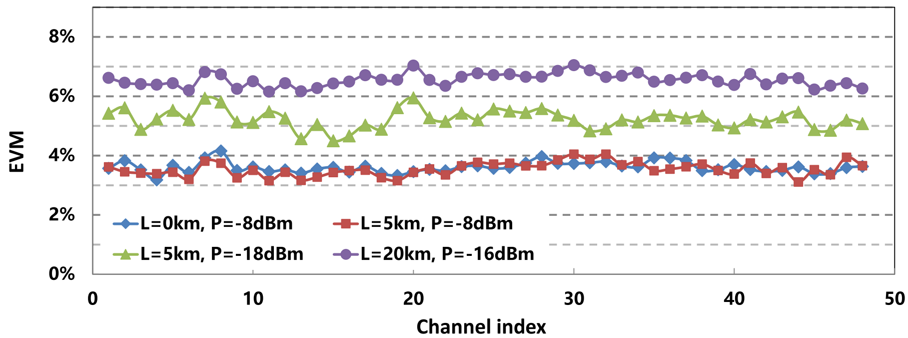

Fig. 6. EVMs of all 48 aggregated LTE signals via CDM under (1) L = 0 km, P = −8 dBm, (2) L = 5 km, P = −8 dBm, (3) L = 5 km, P = −18 dBm and (4) L = 20 km, P = −16 dBm, respectively.

−23 dBm. The representative recovered OFDM-64 QAM constellations for received optical power P = −10 dBm and L = 5 km are shown in inset of Fig. 5(a). After 20-km SSMF transmission, almost the same penalty of around 3.6 dB for the requirement of received optical power is observed for both CDM and FDM scheme. To obtain an EVM of below 8%, the required received optical power needs to be higher than −19.8 dBm.

Then, we measure the EVMs of all 48 aggregated LTE signals via CDM under four typical conditions, (1) L = 0 km at P = −8 dBm, (2) L = 5 km at P = −8 dBm, (3) L = 5 km at P = −18 dBm and (4) L = 20 km at P = −16 dBm. As shown in Fig. 6, all the 48 signals have similar EVM values, indicating of reasonable performance uniformity in the code domain. Moreover, the fronthaul performances under the condition of 5-km SSMF reach are very similar to the case of B2B transmission. The signal EVMs after 5-km SSMF transmission with P = −18 dBm and 20-km SSMF transmission with P = −16 dBm are ∼5.1% and ∼6.6%, respectively, which is well below the 8% EVM threshold specified for 64-QAM.

According to the code theory of orthogonal sequences, there is no multiple-access interferences (MAIs) of undesired channels after synchronous transmission using Walsh code [9]. Therefore, the CDM based fronthaul system using 128-order Walsh codes can theoretically accommodate 64 channels (each channel assigned two orthogonal codes for in-phase/quadrature (I/Q) components). However, with the increase of channel numbers, the transmission power assigned to the desired LTE channel will decrease at a given total transmission power. The effect of background noise becomes relatively larger. Therefore, the transmission performance will be degraded [19]. To identify the source of performance penalty and evaluate the maximum number of channels that can be accommodated using CDM, we measure the mean EVM versus the number of aggregated channels, under (1) L = 0 km, P = −6 dBm, (2) L = 5 km, P = −6 dBm, (3) L = 20 km, P = −6 dBm and (4) L = 20 km, P = −16 dBm, respectively. Without loss of generality, the code index is $\{1, 2, 3 \ldots 2M\text{-}1, 2M\}$, where $M \leq 64$ denotes the number of aggregated channels. As shown in Fig. 7, with the increase of channel numbers, EVM performance degradation is found. For example, when L = 20 km, P = −16 dBm, the EVM is ∼7.6% for M = 64, indicating of around 1.8% and 2.2% EVM degradation in comparison with M = 36, and M = 2, respectively. Thus, the maximum number of channels that can be accommodated satisfying an EVM of 8% is 64 under this condition.

By applying the CDM-based channel aggregation for the synchronous 5km transmission of 32 × 20 MHz-LTE signals and 491.52Mbaud-16 QAM CWs, we evaluate the performance, as shown in Fig. 8. Fig. 8(a) shows the measured RF spectrum of the received aggregated LTE signals and CWs before channel de-aggregation, when the received optical power is –8 dBm. Both the LTE signals and CWs share the same spectral bandwidth within ∼1.96 GHz, and the power difference of spectrum is mainly due to the characteristics of different arranged Walsh codes. Fig. 8(b) shows the measured constellations of the 16-QAM signal for the purpose of CWs delivery and the LTE OFDM-64 QAM signals under the same condition. Obviously, the recovered constellations are

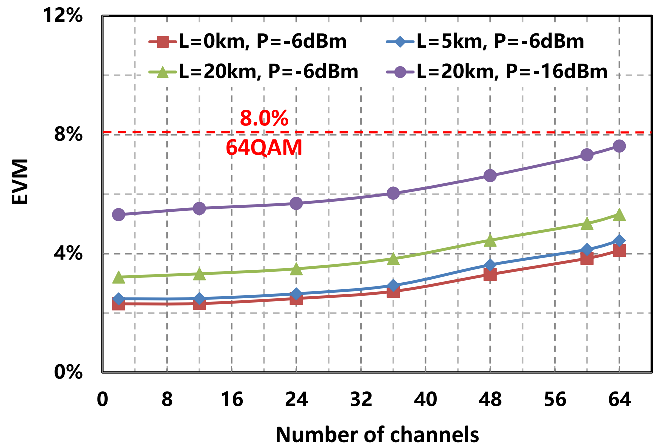

Fig. 7. Mean EVM versus the number of aggregated channels, under (1) L = 0 km, P = −6 dBm, (2) L = 5 km, P = −6 dBm, (3) L = 20 km, P = −6 dBm and (4) L = 20 km, P = −16 dBm, respectively.

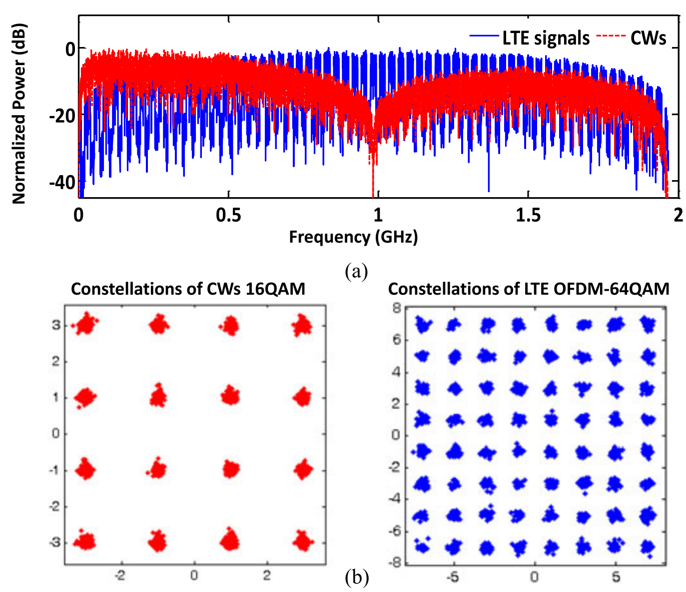

Fig. 8. (a) Measured RF spectrum of the LTE signals and CWs prior to channel de-aggregation at a received optical power of −8 dBm. (b) Measured constellations of the 16-QAM CW signal and the LTE OFDM-64 QAM signals after 5-km SSMF transmission at a received optical power of −8 dBm.

of high quality, and no errors are measured with over 10 million bits processed for the LTE signals and the 16-QAM signal.

Finally, we measure the SNR versus the received optical power for the 491.52-Mbaud 16-QAM signal and the mean EVM of all the 32 × 20-MHz LTE OFDM-64 QAM signals with respect to the received optical power, respectively. The received SNR is measured from the recovered signal constellation, and needs to be over 25 dB to achieve a BER of below 10−12 [8]. As shown in Fig. 9(a), when the received power is more than −22 dBm, no error occurs, and the measured SNRs are all above 25 dB. Meanwhile, the received optical power needs to be larger than −23 dBm, in order to reach the required EVM threshold of 8% for 64-QAM, as shown in Fig. 9(b). We can conclude that both the LTE signals and CWs can be successfully transmitted over the CDM-based fronthaul link with sufficient loss budget in wavelength-division multiplexed passive optical network (WDM-PON) [16].

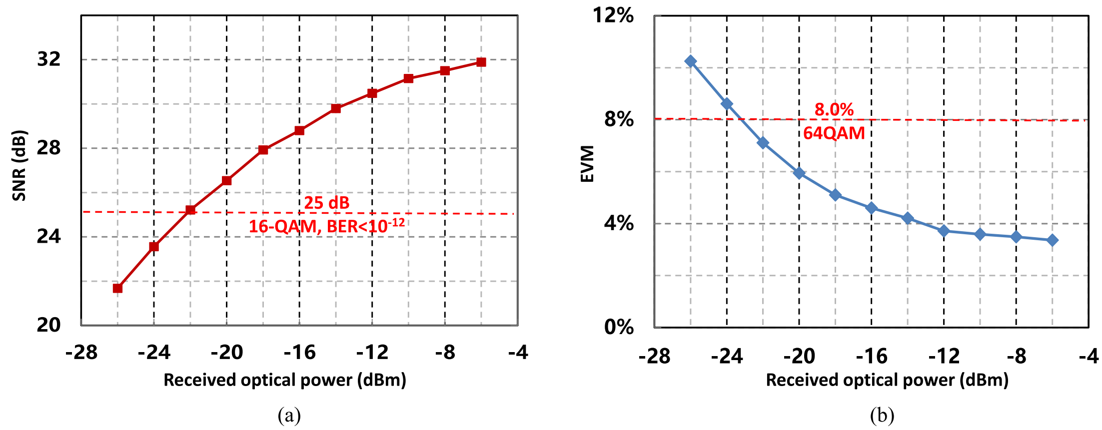

Fig. 9. (a) Measured SNR versus received optical power for the 491.52-Mbaud 16-QAM CW signal; (b) measured EVMs of the 32 × 20-MHz LTE OFDM-64 QAM signals versus received optical power.

5. Conclusion

A novel bandwidth efficient and low-complexity mobile fronthaul architecture via CDM-based digital channel aggregation has been proposed for C-RAN infrastructure. Compared to the FDM based aggregation scheme, the FFT/IFFT operations were replaced by simple sign selection and addition, leading to the significant reduction of computational complexity. To facilitate the control and management of the fronthaul equipment compliant with CPRI, the scheme for synchronous transmission of both the LTE signals and the CWs has also been examined. The proposed MFH architectures have been experimentally demonstrated by either aggregating 48 × 20-MHz LTE signals or 32 × 20-MHz LTE signals together with 491.6 Mbaud CWs over single-wavelength channel with analog bandwidth of 1.966-GHz, respectively. An average EVM of ∼3.6 % is achieved after transmission over 5-km SSMF, while the CWs can be recovered without error.

References

[1] Y. Okumura and J. Terada, "Optical network technologies and architectures for backhaul/fronthaul of future radio access supporting big mobile data," in *Proc. Opt. Fiber Commun. Conf. Opt. Soc. Amer.*, San Francisco, CA, USA, 2014, Paper Tu3F.1.

[2] A. Pizzinat, P. Chanclou, T. Diallo, and F. Saliou, "Things you should know about fronthaul," *J. Lightw. Technol.*, vol. 33, no. 5, pp. 1077–1083, Mar. 2015.

[3] N. Cvijetic, A. Tanaka, K. Kanonakis, and T. Wang, "SDN-controlled topology-reconfigurable optical mobile fronthaul architecture for bidirectional CoMP and low latency inter-cell D2D in the 5G mobile era," *Opt. Express*, vol. 22, no. 17, pp. 20809–20815, 2014.

[4] CPRI Specification V7.0, "Common public radio interface (CPRI); interface specification," 2015.

[5] S. Cho, H. Park, H. Chung, K. Doo, S. Sang, and J. Lee, "Cost-effective next generation mobile fronthaul architecture with multi-IF carrier transmission scheme," in *Proc. Opt. Fiber Commun. Conf. Opt. Soc. Amer.*, San Francisco, CA, USA, 2014, Paper Tu2B.6.

[6] X. Liu, N. Chand, F. Effenberger, L. Zhou, and H. Lin, "Demonstration of bandwidth-efficient mobile fronthaul enabling seamless aggregation of 36 E-UTRA-like wireless signals in a single 1.1-GHz wavelength channel," in *Proc. Opt. Fiber Commun. Conf. Opt. Soc. Amer.*, Los Angeles, CA, USA, 2015, Paper M2J.2.

[7] X. Liu, H. Zeng, N. Chand, and F. Effenberger, "Experimental demonstration of high-throughput low-latency mobile fronthaul supporting 48 20-MHz LTE signals with 59-Gb/s CPRI-equivalent rate and 2-μs processing latency," in *Proc. Eur. Conf. Opt. Commun.*, Valencia, Spain, 2015, Paper We.4.4.3.

[8] X. Liu, H. Zeng, N. Chand, and F. Effenberger, "Efficient mobile fronthaul via DSP-based channel aggregation," *J. Lightw. Technol.*, vol. 34, no. 6, pp. 1556–1564, Mar. 2016.

[9] R. Pickholtz, D. Schilling, and L. Milstein, "Theory of spread-spectrum communications – A tutorial," *IEEE Trans. Commun.*, vol. COM-30, no. 5, pp. 855–884, May 1982.

[10] J. Yue *et al.*, "Network code division multiplexing for wireless relay networks," *IEEE Trans. Wireless Commun.*, vol. 14, no. 10, pp. 5736–5749, Jun. 2015.

[11] X. Wang, Y. Huang, Y. Lu, Y. Yu, and L. Li, "A digital coherent optical code division multiplexing network with 16-Tb/s (2560x6.25-Gb/s) capacity," in *Proc. Eur. Conf. Opt. Commun.*, Dusseldorf, Germany, 2016, pp. 1–3.

[12] J. Fernandez, J. Ingham, R. Penty, and I. White, “18 Gchips/s Electronic CDMA for low-cost optical access networks,” *J. Lightw. Technol.*, vol. 27, vol. 3, pp. 306–313, Feb. 2009.

[13] A. Rizaner, H. Amca, K. Hacioglu, and A. Ulusoy, “Channel estimation by using short training sequences in CDMA systems,” *Wireless Pers. Commun.*, vol. 34, no. 4, pp. 359–371, 2005.

[14] K. Yasuhiro, I. Hideyuki, T. Hideaki, S. Masahiro, and K. Masayuki, “Demonstration of 1.25 Gb/s $\times$ 8-channels ECDM using eight-chip electrical coding,” *IEEE Photon. Technol. Lett.*, vol. 22, no. 12, pp. 875–877, Jun. 2010.

[15] X. Liu, H. Zeng, and F. Effenberger, “Bandwidth-efficient synchronous transmission of I/Q waveforms and control words via frequency-division multiplexing for mobile fronthaul,” in *Proc. IEEE Global Commun. Conf.*, San Francisco, CA, USA, 2016, Paper SAC 21-3.

[16] D. Nesset, “NG-PON2 technology and standards,” *J. Lightw. Technol.*, vol. 33, no. 5, pp. 1136–1143, Mar. 2015.

[17] K. Alameh and R. A. Minasian, “Optimum optical modulation index of laser transmitters in SCM systems,” *IET Electron. Lett.*, vol. 26, no. 16, pp. 1273–1275, 1990.

[18] M. Bodrato, “Towards optimal Toom-Cook multiplication for univariate and multivariate polynomials in characteristic 2 and 0,” in *International Workshop on Arithmetic of Finite Fields*, vol. 4547. Berlin, Germany: Springer-Verlag, 2007, pp. 116–133.

[19] H. Rowe, “Bounds on the number of signals with restricted cross correlation,” *IEEE Trans. Commun.*, vol. COM-30, no. 5, pp. 966–974, May 1982.